Magnetization reversal in individual micrometer-sized polycrystalline Permalloy rings

T. A. Moore, T. J. Hayward, D. H. Y. Tse, J. A. C. Bland, F. J. Castaño, and C. A. Ross

Citation: Journal of Applied Physics **97**, 063910 (2005); doi: 10.1063/1.1858055
View online: https://doi.org/10.1063/1.1858055
View Table of Contents: http://aip.scitation.org/toc/jap/97/6
Published by the American Institute of Physics

Magnetization reversal in individual micrometer-sized polycrystalline Permalloy rings

T. A. Moore, T. J. Hayward, D. H. Y. Tse, and J. A. C. Bland
Cavendish Laboratory, University of Cambridge, Cambridge CB3 0HE, United Kingdom

F. J. Castaño and C. A. Ross
Department of Materials Science and Engineering, Massachusetts Institute of Technology, Cambridge, Massachusetts 02139

(Received 1 October 2004; accepted 16 December 2004; published online 14 March 2005)

The magnetization reversal of individual 2 μm and 5 μm diameter polycrystalline Permalloy rings, with respective widths 0.75 μm and 1 μm, thickness 45 nm, has been investigated by focused magneto-optic Kerr effect (MOKE) magnetometry. Micromagnetic simulation of the reversal in the 2 μm diameter ring reveals that the onion-to-vortex state switching occurs by nucleation and subsequent annihilation of vortex walls that span the width of the ring, and that the vortex-to-reverse-onion state switching occurs by expansion of a reverse domain. The hysteresis loop shows good agreement with the experimental MOKE loop. Measurements of the switching through one-half of a 5 μm diameter ring enable the determination of the circulation of the vortex states accessed during one applied field cycle. The rings switch via one vortex state (either clockwise or anticlockwise) on both downward and upward applied field sweeps. The number of applied field cycles spent switching via one vortex state before changing to switch via the opposite vortex state is random, likely to be due to the history of the spin configuration and thermal fluctuations. © *2005 American Institute of Physics*. [DOI: 10.1063/1.1858055]

I. INTRODUCTION

Thin film ferromagnetic ring structures are currently the subject of intensive study due to their potential for use in memory and sensor devices.[1,2] In a technological application, it would be an advantage for the ring structures to exhibit reproducible transitions between stable, well-defined magnetization states. Several magnetization states have been identified in micrometer-sized cobalt and Permalloy rings, including the onion, vortex, vortexcore, and twisted states.[3–5] Whether these states arise depends on geometrical parameters, such as ring thickness and width, which determine the stability of a spin configuration in a given field range via a magnetostatic energy contribution. The magnetization reversal can thus range from a very simple single switching in thin rings to a more complex triple switching in thick, wide rings.

To determine the suitability of a particular ring geometry for a device, it is necessary to measure the magnetization reversal in an individual ring. Several methods have been used to measure magnetization reversal collectively from an array of ring structures, including magneto-optic Kerr effect (MOKE),[4] photoemission electron microscopy (PEEM),[5] magnetic force microscopy (MFM),[3] and superconducting quantum interference device.[6] These are "averaging" techniques that do not account for the variation in switching fields that arise from small differences in size and edge roughness between the rings. Some techniques such as scanning electron microscopy with polarization analysis,[5] magnetoresistance,[7] and local Hall effect (LHE),[8,9] as well as MFM and PEEM, can probe magnetization reversal in a single ring. However, for a noninvasive, direct measurement of a hysteresis loop from a single ring, MOKE and LHE are the main candidates, MOKE having the potential for spatial resolution <200 nm on ultrafast time scales.[10] In this work we demonstrate hysteresis loop measurement by MOKE from single 2 μm and 5 μm diameter 45 nm thick Permalloy rings and compare the former with a micromagnetic simulation. The rings switch from onion-to-reverse-onion state via a vortex state which may be of either clockwise or anticlockwise circulation. By making MOKE measurements of the switching through one half of a ring we are able to determine the circulation of the intermediate vortex state.

II. EXPERIMENT

The Permalloy ($Ni_{80}Fe_{20}$) ring arrays were fabricated using a combination of electron beam lithography and lift-off processing. Polymethyl-methacrylate was spun to a thickness of 200 nm onto a thermally oxidized 3 in. diameter Si(100) wafer. The ring patterns were written by scanning the electron beam along parallel single-pixel circular trajectories using a Raith-150 electron beam lithography system. The number of single-pixel lines in the ring patterns defined the width of the structure. The resist was then developed in a 2:1 solution of isopropyl alcohol and methylisobutylketone at a temperature of 21 °C for 90 s. Subsequently a layer of Permalloy of thickness 45 nm was electron beam evaporated onto the patterned resist. Finally the resist together with the unwanted Permalloy was removed by dipping the sample in n-methylpyrrolidone at 120 °C, followed by an ultrasonic bath. The ring arrays were covered with 3 nm of Au to prevent oxidation.

Permalloy was chosen in order to give a low switching field suitable for measurement in our focused MOKE magnetometer. The 45 nm continuous Permalloy film had a coercive field of 3 Oe. One array contained rings of 5 μm outer

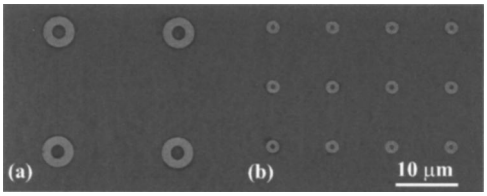

FIG. 1. Scanning electron microscopy images of polycrystalline Permalloy rings: (a) part of an array of 5 μm diameter rings, (b) part of an array of 2 μm diameter rings. The scale bar applies to both (a) and (b), and the magnification is 3000 times.

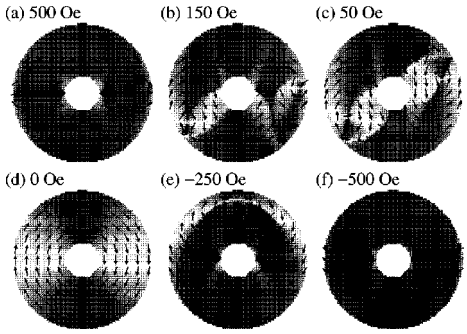

FIG. 2. Spin configurations of the 2 μm diameter polycrystalline Permalloy ring at different stages in the micromagnetic simulation. The $+x$ direction is to the right. (a) Initial onion state in the $+x$ direction. (b) Two vortex domain walls, clockwise and anticlockwise, are nucleated in an asymmetric spin configuration. (c) The vortex walls expand and the anticlockwise vortex wall moves away from the x axis. (d) The vortex state is formed after the two vortex walls annihilate one another. (e) The area of magnetic moments pointing in the $-x$ direction expands and an arcing domain wall of transverse character separates $-x$- and $+x$-directed spins. (f) The reverse onion state forms.

diameter, 1 μm width, and 20 μm repeat distance, another contained rings of 2 μm outer diameter, 0.75 μm width, and 10 μm repeat distance. In addition to the main study, 20 μm diameter rings of width 5 μm and repeat distance 50 μm were fabricated and investigated. Figure 1 shows scanning electron microscope images of part of an array of 5 μm diameter rings (a) and part of an array of 2 μm diameter rings (b). Hysteresis loops were measured from the rings collectively using a conventional MOKE magnetometer in the longitudinal configuration, with the laser spot covering the entire array (area $\sim 200\times 200$–300×300 μm^2). Subsequently, hysteresis loops were measured from individual rings using a focused MOKE magnetometer. Here, the laser spot is focused by a 20X Zeiss microscope objective lens to an area that just encapsulates the ring. The applied field was cycled sinusoidally in time at a frequency of ~ 2 Hz with amplitude sufficient to reach the onion state at the end of each upward and downward sweep. The average of several hundred hysteresis loops was captured. Finally, the laser spot was focused even further (~ 2 μm diameter) until it covered the width of one 5 μm diameter ring at the halfway point between the two 180° domain walls in the onion state. Cycling the applied field sinusoidally as before, the magnetization switching in the probed area could be measured as a function of field.

A micromagnetic simulation of the hysteresis loop in a 2 μm diameter polycrystalline Permalloy ring was made using the publicly available Object Oriented Micromagnetic Framework program with parameters of saturation magnetization $M_S = 800\times 10^3$ A m^{-1}, exchange constant $A = 1.3\times 10^{-11}$ J m^{-1}, anisotropy constant $K = 0$, cell size 4 nm, and damping $\alpha = 0.5$. The applied field was reduced from 500 to −500 Oe in steps of 5 Oe, giving one branch of the hysteresis loop, the other half being inferred by symmetry.

III. RESULTS AND DISCUSSION

Figure 2 shows spin configurations of the 2 μm diameter polycrystalline Permalloy ring at different stages in the micromagnetic simulation. Initially, the majority of magnetic moments are pointing in the $+x$ direction, giving the onion state shown in (a). As the applied field is reduced (b), two vortex walls are nucleated in an asymmetric configuration, one clockwise and the other anticlockwise. The reason for the asymmetric spin configuration in a nominally symmetric micromagnetic problem is currently unknown, but could be due either to rounding errors in the calculation, or to the fact that an integral number of cell sizes does not fit into the ring width, or both. The large width of the ring favors the formation of vortex walls over transverse walls, as the reduction in magnetostatic energy more than compensates for the increase in exchange energy. Further reduction of the applied field (c) allows the vortex walls to expand to cover the width of the ring (0.75 μm), and the anticlockwise vortex wall to move a short distance around the ring in an anticlockwise direction. At zero applied field [remanence (d)] the vortex state is present, and is reached when the clockwise vortex wall moves around the ring to annihilate with the anticlockwise vortex wall. The asymmetry in the movement of the vortex walls, leading in this case to a clockwise vortex state rather than an anticlockwise vortex state, is assumed to originate from the asymmetry in the spin configuration at (b). The vortex-to-onion transition in negative applied fields (e) starts by expansion of the region of magnetic moments pointing in the $-x$ direction. An arcing domain wall of transverse character separates the $-x$- and $+x$-directed spins in the top half of the ring. Eventually the $+x$-directed domain is pushed out and the reverse onion state is reached (f).

The simulated hysteresis loop branch from positive to negative x-directed magnetization M_x for the 2 μm diameter polycrystalline Permalloy ring is shown in Fig. 3. Schematic diagrams show the spin configuration at each stage. There are two major transitions labeled H_{c1} and H_{c2} and three small jumps. The first small jump at 187.5 Oe occurs when the two vortex domain walls are nucleated. The second small jump at 82.5 Oe occurs when the vortex walls grow larger and move in an anticlockwise direction a short distance around the ring. As the field is reduced, $H_{c1} = 22.5$ Oe marks the transition into the vortex state, when the vortex walls annihilate one another. The second major transition is at $H_{c2} = -232.5$ Oe when the region of $-x$-directed spins expands into the upper half of the ring. Finally, a third small jump occurs at −312.5 Oe when remaining $+x$-directed spins are reversed, leaving the reverse onion state.

The simulated hysteresis loop corresponds well with the hysteresis loop measured from a single 2 μm diameter Permalloy ring [Fig. 4(a)]. Although the three small jumps are

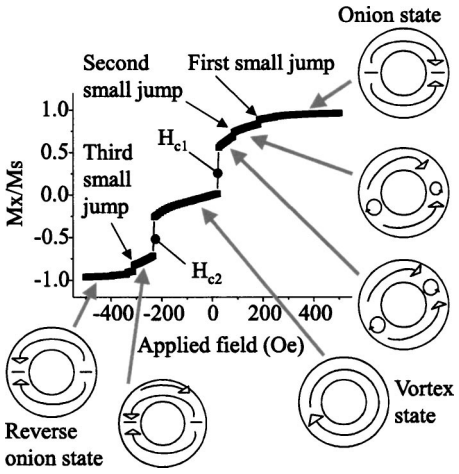

FIG. 3. Micromagnetic simulation of the hysteresis loop branch from positive to negative M_x for the 2 μm diameter polycrystalline Permalloy ring. Schematic diagrams show the spin configuration at each stage. The simulation started at 500 Oe and the *x*-directed applied field was reduced in steps of 5 Oe.

not distinguishable, the two major transitions occur at very similar values of H_{c1} and H_{c2} ($\sim$20 Oe and ~ -230 Oe, respectively). The hysteresis loop measured from the array of 2 μm diameter Permalloy rings [Fig. 4(b)] gives the same values of H_{c1} and H_{c2} within error (20 ± 40 Oe and -260 ± 40 Oe). The differences between this measurement and the experimental loop in Fig. 4(a) are that the signal-to-noise ratio is improved due to the larger probed area and that the transitions are less abrupt due to the averaging of switching fields H_{c1} and H_{c2} over several ring structures. The hysteresis loop of the array of 5 μm diameter Permalloy rings is shown in Fig. 4(c). An important difference between the 5 μm and 2 μm diameter rings is that the larger ring does not reach the vortex state at zero applied field, i.e., it has a net magnetization at remanence. H_{c1} and H_{c2} are both negative, -20 ± 20 Oe and -130 ± 20 Oe, respectively. The change of sign of H_{c1} and the increase of H_{c2} as the ring width is decreased mimic the behavior seen in 2 μm diameter Permalloy rings[9] and 1 and 2 μm diameter cobalt rings.[11]

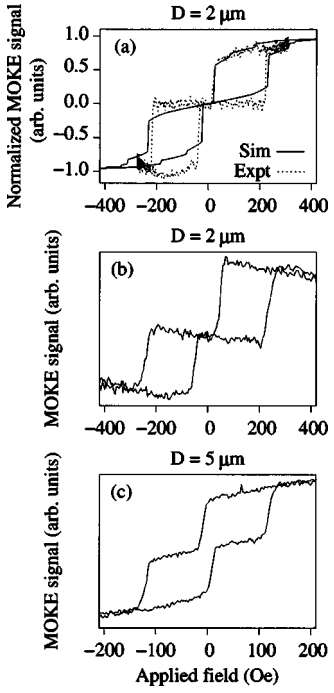

FIG. 4. (a) Comparison of simulated hysteresis loop (Sim) with normalized experimental MOKE data (Expt) for a single 2 μm diameter polycrystalline Permalloy ring. (b) and (c) Hysteresis loops measured by MOKE from arrays of 2 μm and 5 μm diameter polycrystalline Permalloy rings, respectively.

Nine 5 μm and nine 2 μm diameter rings were measured separately in each array. For the smaller rings, the H_{c1} and H_{c2} distributions both have a span of 14–15 Oe, whereas for the larger rings the H_{c1} distribution has a shorter span (10 Oe) than the H_{c2} distribution (25 Oe). The variations of switching field arise from small differences in size and edge roughness between individual rings, which give local differences in domain wall pinning strength and energy barriers to nucleation. Hysteresis loops from the array of 20 μm diameter rings show the same features as the smaller structures, and in particular a small jump may be observed before the first major transition at H_{c1} that could be related to the nucleation of vortex walls seen in the simulation (Fig. 3).

The final measurement demonstrates the ability of our focused MOKE magnetometer to determine the magnetization reversal properties of individual 5 μm diameter Permalloy rings over several cycles of the applied field, and in particular the circulations of the vortex states on a given cycle. The laser was focused to a ~ 2 μm diameter spot covering the width of a 5 μm diameter polycrystalline Permalloy ring at the halfway point between the two 180° domain walls in the onion state. This is illustrated schematically in Fig. 5 by a dashed circle on the ring. The magnetization as a function of applied field was then measured during several consecutive field cycles. To understand the results of this measurement it is first necessary to understand how the switching is distributed spatially in the ring during a reversal of the field. Starting in the onion state, the first transition at H_{c1} occurs when one of the 180° domain walls sweeps through one side of the ring and annihilates the other wall, giving rise to a vortex state. Considering the diagram of the onion state in Fig. 3 it is clear that there are four possible ways in which this transition can occur: (i) left wall sweeps through top half of ring, (ii) left wall sweeps through bottom half of ring, (iii) right wall sweeps through top half of ring, and (iv) right wall sweeps through bottom half of ring. In cases (i) and (iii) an anticlockwise vortex state is formed, and in cases (ii) and (iv) a clockwise vortex state is formed. The switch from the vortex state to the reverse onion state, which occurs by growth of a reverse domain, will then naturally take place in the side of the ring not switched at H_{c1}. By measuring the magnetization in one half of the ring during reversal of the field, we observe one of the two possible transitions [onion-to-vortex (O-V) at H_{c1} or vortex-to-onion (V-O) at H_{c2}], and can therefore determine which vortex state (clockwise or anticlockwise) is formed.

Figure 5 shows examples of all the possible hysteresis loops (and corresponding switching routes) that may result from one complete cycle of the applied field. In the first loop, labeled O-V V-O, the onion-to-vortex transition during the first half of the applied field cycle occurs in the side of the

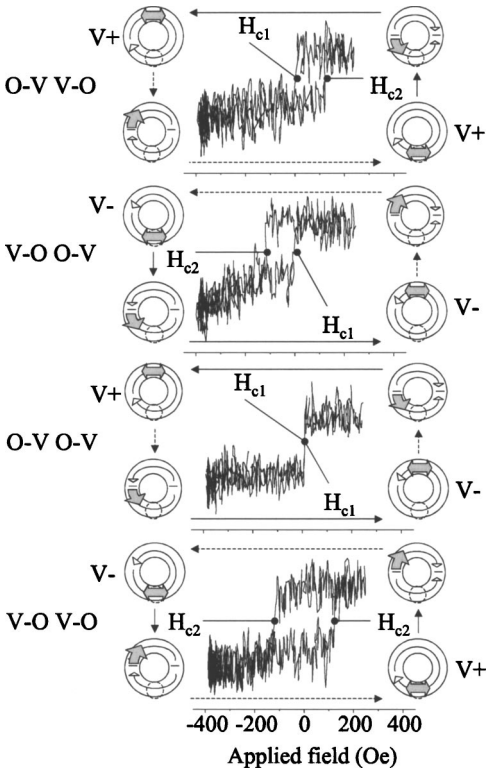

FIG. 5. Schematic diagrams and hysteresis loops illustrating the four possible switching routes of a 5 μm diameter polycrystalline Permalloy ring during one cycle of the applied field. The dashed circle on the lower half of the ring in the diagrams is the area covered by the laser spot. The single-headed block arrows represent movement of a 180° domain wall (onion-to-vortex transition O-V). The double-headed block arrows represent growth of a reverse domain (vortex-to-onion transition V-O). The solid-line arrows represent transitions that are observed at the laser spot, whilst the dashed-line arrows represent transitions that take place unobserved on the opposite side of the ring. On route O-V V-O an onion-to-vortex transition followed by a vortex-to-onion transition is seen at the laser spot. Route V-O O-V is the opposite of O-V V-O. On route O-V O-V two onion-to-vortex transitions are seen at the laser spot, while on route V-O V-O two vortex-to-onion transitions are seen. O-V transitions occur at H_{c1} close to zero field, while V-O transitions occur at a higher field H_{c2}, as indicated by the hysteresis loops. V+ represents a clockwise intermediate vortex state and V− an anticlockwise intermediate vortex state.

ring where the laser spot is located and hence the first switch of the hysteresis loop is at H_{c1} (O-V). As the ring is switched back from the reverse onion state, the onion-to-vortex transition occurs in the side of the ring not under observation and hence the second switch of the hysteresis loop is at H_{c2}, representing the high field V-O transition. In the second loop, labeled V-O O-V, the opposite situation occurs in that the V-O transition at H_{c2} is observed in the first switch of the loop and the O-V transition at H_{c1} is observed in the second switch. The two remaining loops result when the onion-to-vortex transition occurs in the same side of the ring during both halves of the applied field cycle. The loop labeled O-V O-V is recorded when the onion-to-vortex transition occurs in the observed half of the ring, and the loop labeled V-O V-O is recorded when the onion-to-vortex transition occurs in the unobserved half of the ring.

It can be seen in Fig. 5 that the switching routes that yield the same vortex state during both halves of the applied field cycle are O-V V-O and V-O O-V. On these switching routes the vortex states are uniformly clockwise (V+) and anticlockwise (V−), respectively. Observing the magnetization switching in a half ring over several consecutive cycles of the applied field, we find that the switching routes O-V V-O and V-O O-V are vastly preferred over the switching routes O-V O-V and V-O V-O. In other words the rings switch via one vortex state (either clockwise or anticlockwise) both forwards and backwards. Additionally, the rings spend a variable number of field cycles switching via one vortex state before randomly changing to switch via the other. The switching routes O-V O-V and V-O V-O only appear to exist as transitions between the preferred routes O-V V-O and V-O O-V. We measured the circulation of the vortex state over 50 consecutive field cycles for three different 5 μm diameter Permalloy rings. One of the rings oscillates between the switching routes O-V V-O and V-O O-V [characterized by a clockwise (V+) and an anticlockwise (V−) vortex state, respectively] five times over the course of 50 field cycles. A second ring spends 32 field cycles following the route O-V V-O before oscillating three times in quick succession and finally ending on the V-O O-V route. A third ring also spends more field cycles following route O-V V-O but oscillates at more regular intervals. These results emphasize the differences in magnetization reversal characteristics between the nominally identical 5 μm diameter rings. The switching route (i.e., switching via clockwise or anticlockwise vortex state) is randomly determined and likely to be influenced by the history of the spin configuration as well as by thermal fluctuations, which bias the 180° domain walls to sweep through one side of the ring or the other. Local shape irregularities could also affect the spin configuration, biasing the ring to switch in a particular way and giving rise to differences in magnetization reversal characteristics between individual rings.

IV. CONCLUSION

In this work we have measured the magnetization reversal in individual micrometer-sized polycrystalline Permalloy rings using a focused MOKE magnetometer. Specifically, we have captured hysteresis loops from single 2 μm and 5 μm diameter rings of thickness 45 nm and respective widths 0.75 μm and 1 μm. For the 2 μm diameter ring, the experimental loop corresponded well with the loop resulting from a micromagnetic simulation. The simulation reveals that the onion-to-vortex state switching occurs by nucleation and subsequent annihilation of vortex walls that span the width of the ring, and that the vortex-to-reverse-onion state switching occurs by expansion of a reverse domain. Measurement of individual rings highlights the variation of the switching fields H_{c1} and H_{c2} for the onion-to-vortex and vortex-to-onion transitions, which is the result of small differences in size and edge roughness between rings. Focused MOKE measurements of the magnetization switching through one half of a 5 μm diameter ring allows the determination of the circulation of the vortex states accessed during one applied field cycle. The rings switch via one vortex state (either clockwise or anticlockwise) on both downward and upward applied field sweeps. The number of applied field cycles spent switching

via one vortex state before changing to switch via the opposite vortex state is random, likely to be due to the history of the spin configuration and thermal fluctuations. For the integration of thin film ferromagnetic rings into devices, the information provided by focused MOKE measurements could be critical.

ACKNOWLEDGMENT

The authors are grateful for the support of the Cambridge-MIT Institute.

[1]X. Zhu and J.-G. Zhu, IEEE Trans. Magn. **39**, 2854 (2003).
[2]M. M. Miller, G. A. Prinz, S.-F. Cheng, and S. Bounnak, Appl. Phys. Lett. **81**, 2211 (2002).
[3]F. J. Castano, C. A. Ross, C. Frandsen, A. Eilez, D. Gil, H. I. Smith, M. Redjdal, and F. B. Humphrey, Phys. Rev. B **67**, 184425 (2003).
[4]J. Rothman, M. Klaui, L. Lopez-Diaz, C. A. F. Vaz, A. Bleloch, J. A. C. Bland, Z. Cui, and R. Speaks, Phys. Rev. Lett. **86**, 1098 (2001).
[5]M. Klaui *et al.*, Phys. Rev. B **68**, 134426 (2003).
[6]M. Klaui *et al.*, Appl. Phys. Lett. **84**, 951 (2004).
[7]M. Klaui, C. A. F. Vaz, J. Rothman, J. A. C. Bland, W. Wernsdorfer, G. Faini, and E. Cambril, Phys. Rev. Lett. **90**, 097202 (2003).
[8]J. Bekaert, D. Buntinx, C. Van Haesendonck, V. V. Moshchalkov, J. De Boeck, G. Borghs, and V. Metlushko, Appl. Phys. Lett. **81**, 3413 (2002).
[9]M. Steiner and J. Nitta, Appl. Phys. Lett. **84**, 939 (2004).
[10]D. A. Allwood, G. Xiong, M. D. Cooke, and R. P. Cowburn, J. Phys. D **36**, 2175 (2003).
[11]M. Klaui, L. Lopez-Diaz, J. Rothman, C. A. F. Vaz, J. A. C. Bland, and Z. Cui, J. Magn. Magn. Mater. **240**, 7 (2002).